

# Entanglement of condensed magnons via momentum-space fragmentation

Clement H. Wong<sup>1,2</sup> and Ari Mizel<sup>2</sup>

<sup>1</sup>*Department of Physics, University of Maryland, College Park, Maryland 20742, USA*

<sup>2</sup>*Laboratory for Physical Sciences, 8050 Greenmead Drive, College Park, Maryland 20740, USA*

(Received 23 March 2017; revised manuscript received 26 May 2017; published 9 August 2017)

A scheme is presented for engineering momentum-space entanglement of fragmented magnon condensates. We consider easy-plane frustrated antiferromagnets in which the magnon dispersion has degenerate minima that represent “umbrella” chiral spin textures. We tune the Hamiltonian near a quantum critical point that is signaled by a singularity in the entanglement entropy. The ground state develops momentum-space entanglement of the chiral spin textures. The size of the entangled superposition is accessible experimentally through the magnetic structure factor. Our model is motivated by equilibrium magnon condensates in frustrated antiferromagnets such as CsCuCl<sub>3</sub>, and it can also be simulated in spin-orbit coupled Mott insulators in atomic optical lattices and circuit quantum electrodynamics.

DOI: [10.1103/PhysRevB.96.054412](https://doi.org/10.1103/PhysRevB.96.054412)

## I. INTRODUCTION

The possibility of creating superpositions of macroscopically distinct quantum states, or “Schrödinger-cat” states [1], has enthralled physicists since shortly after the invention of quantum mechanics. In addition to stimulating fundamental interest, macroscopically entangled states also have applications in quantum information and metrology. A well-known example is the NOON state, which enables Heisenberg-limited interferometry, motion and magnetic field sensing [2], and quantum error correction against photon loss [3].

Bose-Einstein condensates (BEC’s) are natural systems in which to study macroscopic entanglement due to the large number of particles in the ground state. Superposition of spatially separated or momentum-separated BEC’s has been studied in optical lattices of ultracold atoms [4]. In the solid state, work on macroscopic quantum coherence in magnetic and superconducting materials [5] matured into the realization of coherent superposition of supercurrent states in superconducting flux qubits [6]. Due to their bosonic nature, magnons, or spin waves, can also undergo condensation [7,8]. In this paper, we propose a method to produce a magnon “Schrödinger-cat” state that can exhibit particularly striking entanglement phenomena.

Our proposal creates a superposition of magnon condensates fragmented into two modes at degenerate minima (valleys) in the magnon dispersion of magnetic insulators [9,10]. This type of fragmented BEC can arise in many frustrated antiferromagnetic insulators with degenerate ground states, such as CsCuCl<sub>3</sub>, Cs<sub>2</sub>CuCl<sub>4</sub>, Ba<sub>3</sub>Mn<sub>2</sub>O<sub>8</sub>, and Ba<sub>3</sub>CoSb<sub>2</sub>O<sub>9</sub> [8,11,12]. Specifically, we consider a quasi-two-dimensional canted-XY antiferromagnet (AFM) on a triangular lattice, where easy-plane anisotropy favors ground states with chiral, “umbrella”-type spin textures that can be represented as magnon BEC’s. This lattice naturally appears in the planar spin structure of several quantum magnets, and it can be simulated with engineered spin-orbit-coupled Mott insulators in atomic optical lattices [13] or circuit quantum electrodynamics [14].

This paper is organized as follows. In Sec. II, we summarize the well-known theoretical description of magnetic ordering as a condensation of magnons. In Sec. III, we present our proposal for creating magnon entanglement in the ground state, and we

show that by tuning parameters near a quantum critical point, a sufficiently large gap can be generated to enable ground-state preparation at typical dilution refrigeration temperatures. In Sec. IV, we quantify entanglement in the proposed magnon cat state in terms of the entanglement entropy and quantum Fisher information. In Sec. V, we discuss possible decoherence channels, and we argue that this magnon cat state should be remarkably robust.

## II. MAGNON CONDENSATES

The  $XXZ$  spin  $S$  Heisenberg Hamiltonian on the triangular lattice is given by [8,11]

$$H_0 = J_0 \sum_{\mathbf{r},\nu} [S_{\mathbf{r}}^x S_{\mathbf{r}+\delta_{\nu}}^x + S_{\mathbf{r}}^y S_{\mathbf{r}+\delta_{\nu}}^y + \eta S_{\mathbf{r}}^z S_{\mathbf{r}+\delta_{\nu}}^z] + B_0 \sum_{\mathbf{r}} S_{\mathbf{r}}^z,$$

where  $\mathbf{S}_{\mathbf{r}}$  is the spin operator at  $\mathbf{r}$ ,  $J_0$  and  $\eta J_0$  are the transverse and longitudinal antiferromagnetic exchange interactions,  $\mathbf{r}$  is a Bravais lattice vector, and  $\delta_{\nu} = a(\cos \theta_{\nu}, \sin \theta_{\nu})$  are unit vectors along nearest-neighbor bonds, with  $a$  the lattice constant and  $\theta_{\nu} = \nu\pi/3$ . We have defined  $B_0 = g\mu_B H_0^e$ , where  $H_0^e$  is the applied external magnetic field,  $g$  is the  $g$  factor, and  $\mu_B$  is the Bohr magneton.

Restricting our attention to the case  $S > 1/2$ , we map to a system of bosons using the Holstein-Primakov transformation  $S_{\mathbf{r}}^- = S_{\mathbf{r}}^x - i S_{\mathbf{r}}^y = \sqrt{2S - n_{\mathbf{r}}} b_{\mathbf{r}}$  and  $S_{\mathbf{r}}^z = n_{\mathbf{r}} - S$ , where  $b_{\mathbf{r}}$  are the magnon field operators that satisfy  $[b_{\mathbf{r}}, b_{\mathbf{r}'}^{\dagger}] = \delta_{\mathbf{r},\mathbf{r}'}$ , and  $n_{\mathbf{r}} = b_{\mathbf{r}}^{\dagger} b_{\mathbf{r}}$  is the magnon number operator.<sup>1</sup> In momentum space,  $H_0$  to quartic order in magnon operators becomes ( $\hbar = 1$ )

$$H_0 = \sum_{\mathbf{k}} (\omega_{\mathbf{k}} - \mu) n_{\mathbf{k}} + \frac{1}{2N} \sum_{\mathbf{k},\mathbf{k}'} v_{\mathbf{q}}(\mathbf{k},\mathbf{k}') b_{\mathbf{k}-\mathbf{q}}^{\dagger} b_{\mathbf{k}'+\mathbf{q}}^{\dagger} b_{\mathbf{k}} b_{\mathbf{k}'}, \quad (1)$$

where  $N$  is the number of lattice sites,  $b_{\mathbf{k}}$  are destruction operators,  $\mu = B_s - B_0$  is the effective chemical potential,

<sup>1</sup>For the Holstein-Primakov expansion to be valid, the magnon operators must satisfy the constraint  $n_{\mathbf{r}} \ll 2S$ , but we shall not need to impose this explicitly since  $\langle n_{\mathbf{r}} \rangle \ll 2S$  in our parameter range of interest.

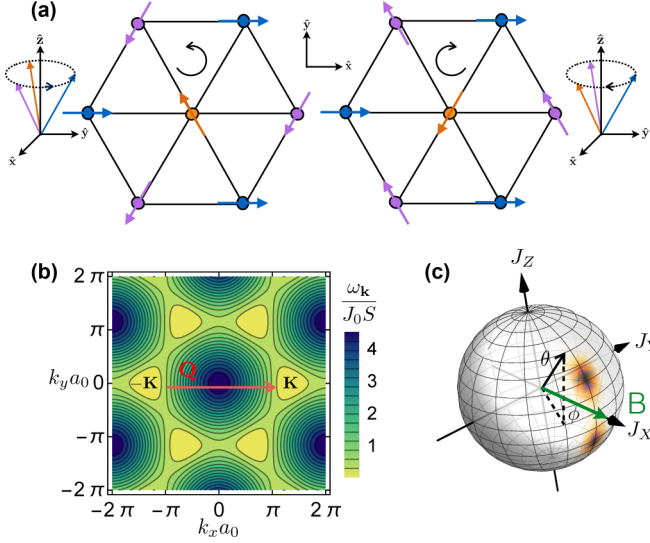


FIG. 1. (a) Chiral “umbrella” spin textures in the degenerate ground states of antiferromagnets on the triangular lattice at zero field. (b) Magnon dispersion with distinct degenerate minima at  $\pm \mathbf{K}$  carrying opposite chiralities. (c) Superposition of the degenerate ground states represented on the Bloch sphere (density plot). North and south poles correspond to magnons completely condensed at  $-\mathbf{K}$  and  $\mathbf{K}$ , respectively. Shown here is the state engineered by coupling the valleys with a sinusoidal field (green arrow) along  $\hat{\mathbf{z}}$  with wave vector  $\mathbf{Q} = 2\mathbf{K}$ .

and  $B_s = 6J_0S(1 + 2\eta)$  is the saturation field. The  $b_{\mathbf{k}}$ 's are defined by  $b_{\mathbf{r}} = \sum_{\mathbf{k}} b_{\mathbf{k}} e^{i\mathbf{k}\cdot\mathbf{r}}/\sqrt{N}$  and satisfy  $[b_{\mathbf{k}}, b_{\mathbf{k}'}^\dagger] = \delta_{\mathbf{k}\mathbf{k}'}$  with  $n_{\mathbf{k}} = b_{\mathbf{k}}^\dagger b_{\mathbf{k}}$ . The Fourier component of the two-body repulsive density-density interaction has the form [15]

$$v_{\mathbf{q}}(\mathbf{k}, \mathbf{k}') = J_0(2\eta\gamma_{\mathbf{q}} - \gamma_{\mathbf{k}} - \gamma_{\mathbf{k}-\mathbf{q}}). \quad (2)$$

The dispersion is given by  $\omega_{\mathbf{k}} = 2J_0S(3 + \gamma_{\mathbf{k}})$ , where  $\gamma_{\mathbf{k}} = \sum_{\mathbf{v}} e^{-i\mathbf{k}\cdot\delta_{\mathbf{v}}}$ . As shown in Fig. 1(b), the dispersion has two inequivalent degenerate minima (valleys). We choose to index them by  $\pm \mathbf{K} = \pm(4\pi/3a, 0, 0)$ . When  $B_0 > |B_s|$  or  $\mu < 0$ , the system's ground state is in the normal phase with fully polarized spins. We will be interested in the case  $B_0 \lesssim |B_s|$  or  $\mu \gtrsim 0$ , when the spins are canted out-of-plane, and one can treat the ground state as a Bose condensate of a dilute Bose gas [8,11]. We note that AFM dimers can also be mapped to the Bose gas Hamiltonian Eq. (1) [8,16].

An approximation to the total Hamiltonian  $H_0$  is obtained by projecting onto the valley states to obtain [9]

$$H = -\left(\mu + \frac{\chi_1}{2}\right)(\hat{n}_{-\mathbf{K}} + \hat{n}_{\mathbf{K}}) + \frac{\chi_1}{2}(\hat{n}_{-\mathbf{K}} + \hat{n}_{\mathbf{K}})^2 + (\chi_2 - \chi_1)\hat{n}_{-\mathbf{K}}\hat{n}_{\mathbf{K}}, \quad (3)$$

where  $\hat{n}_i = b_i^\dagger b_i$ , and  $\chi_1 = v_0(\mathbf{K}, \mathbf{K})/N$  and  $\chi_2 = [v_0(-\mathbf{K}, \mathbf{K}) + v_0(\mathbf{K}, \mathbf{K})]/N$  are the self-interaction and mutual interaction strengths, respectively. We find that  $v_0(-\mathbf{K}, \mathbf{K}) = 6J_0(1 - \eta)$  and  $v_0(\mathbf{K}, \mathbf{K}) = 6J_0(1 + 2\eta)$ . The self-interaction tends to condense magnons into both valleys equally, leading to a “fragmented” BEC in momentum space [10]. The mutual interaction tends to condense magnons into one valley or the other. We consider the case of easy-plane

anisotropy,  $\eta < 1$ , so that  $\chi_2 > \chi_1$ , and the mutual interaction is stronger.<sup>2</sup>

The leading-order ground-state energy is obtained by replacing  $b_{\mathbf{k}}$  with a condensate wave function  $\langle b_{\mathbf{k}} \rangle$ . The ground state is doubly degenerate, consisting of a BEC occupying either  $\mathbf{K}$  or  $-\mathbf{K}$ . The two ground states exhibit “umbrella”-type spin textures

$$\langle \mathbf{S} \rangle = \sqrt{S \left(1 - \frac{B_0}{B_s}\right)} [\cos(\mathbf{K} \cdot \mathbf{r})\hat{\mathbf{x}} \pm \sin(\mathbf{K} \cdot \mathbf{r})\hat{\mathbf{y}}] - S \frac{B_0}{B_s} \hat{\mathbf{z}},$$

where neighboring spins on a triangular plaquette have relative in-plane angles of  $120^\circ$  as shown in Fig. 1(a). Focusing on a given triangular plaquette, one sees that the two ground states exhibit spin textures of opposite chirality.

### III. ENGINEERING ENTANGLEMENT OF MAGNON CONDENSATES

In this paper, we propose engineering quantum superpositions of these two opposite chirality states by introducing a coupling between valleys. This can be achieved via a sinusoidal external magnetic field  $\mathbf{H}_{\mathbf{r}}^e = H^e \cos(\mathbf{Q} \cdot \mathbf{r})\hat{\mathbf{z}}$  with wave vector  $\mathbf{Q} = 2\mathbf{K}$ . Up to a constant, the Zeeman energy adds

$$H_B = -\frac{B}{2}(b_{-\mathbf{K}}^\dagger b_{\mathbf{K}} + b_{\mathbf{K}}^\dagger b_{-\mathbf{K}})$$

to Eq. (3), where  $B = g\mu_B H^e$ . One can understand this coupling classically: due to the alternating direction of the magnetic field, the adjacent spins rotate in opposite directions, causing the oscillations between spin textures of opposite chirality.

Since the total condensate particle number  $n_{-\mathbf{K}} + n_{\mathbf{K}} \equiv 2J$  is a constant of motion, we analyze  $H + H_B$  with fixed  $J$ . To describe quantum coherence between valleys, it is useful to formally regard  $|\mathbf{K}\rangle$  and  $|-\mathbf{K}\rangle$  as pseudospin-up and -down, respectively. We introduce the total valley pseudospin operator using the Schwinger representation for angular momentum  $\mathbf{J} = \vec{b}^\dagger \boldsymbol{\sigma} \vec{b}/2$ , where  $\boldsymbol{\sigma}$  is the vector of Pauli matrices and  $\vec{b} = (b_{-\mathbf{K}}, b_{\mathbf{K}})$ . The operators  $\mathbf{J}$  satisfy the usual angular momentum algebra with  $\mathbf{J}^2 = J(J + 1)$  [17]. The valley polarization operator

$$J_Z = (b_{-\mathbf{K}}^\dagger b_{-\mathbf{K}} - b_{\mathbf{K}}^\dagger b_{\mathbf{K}})/2 \quad (4)$$

defines the eigenstates  $J_Z |J, m\rangle = m |J, m\rangle$ , where  $m = (n_{-\mathbf{K}} - n_{\mathbf{K}})/2$  and  $-J \leq m \leq J$ . We define the pseudospin Hamiltonian  $H_J$  by

$$H + H_B = H_J - 2J(\mu + \chi_1/2) - J^2(\chi_1 + \chi_2),$$

where

$$H_J = -AJ_Z^2 - BJ_X \quad (5)$$

and  $A = \chi_2 - \chi_1 = v_0(-\mathbf{K}, \mathbf{K})/N$ .

The Hamiltonian Eq. (5), viewed as a many-spin system with infinite coordination number, is a limit of the

<sup>2</sup>Quantum corrections to the interaction strengths are suppressed by  $1/S$  [11].

Lipkin-Meshkov-Glick [18–21] model.<sup>3</sup> In the thermodynamic (TD) limit  $J \rightarrow \infty$ , Eq. (5) exhibits a second-order quantum phase transition (QPT) at the critical field  $B_c = 2AJ$  between eigenstates of  $-J_Z^2$  and  $-J_X$ , which are distinguished by the order parameter  $\langle J_X \rangle$ .<sup>4</sup> In the “broken” phase, at  $B < B_c$ ,  $\langle J_X \rangle = B/B_c$ , and the ground state is doubly degenerate and gapless. In the “symmetric” phase, at  $B \geq B_c$ ,  $\langle J_X \rangle = J$ , and the ground state is nondegenerate and gapped.

Rather than focusing on the thermodynamic limit, we seek a finite-size system with (i) an energy gap to excitation sufficiently large to observe the ground state, and (ii) a ground state that manifests macroscopic entanglement. Working in the  $J_Z$  basis  $|J, m\rangle$ , we first numerically compute the ground state  $|\Psi\rangle = \sum_m c_{Jm} |J, m\rangle$  and energy gap of Eq. (5). To develop an understanding of the results, we go to the spin coherent state basis

$$|\theta, \phi\rangle = \frac{1}{(1 + |w|^2)^J} \sum_{m=-J}^J \binom{2J}{J-m}^{1/2} w^{J-m} |J, m\rangle, \quad (6)$$

where  $w = e^{i\phi} \tan \theta/2$  is the stereographic projection of the sphere onto the complex plane. Since Eq. (6) is an eigenstate of  $\mathbf{n} \cdot \mathbf{J}$  with  $\mathbf{n} = (\sin \theta \cos \phi, \sin \theta \sin \phi, \cos \theta)$ , it can be visualized as a point on the pseudospin Bloch sphere, as shown in Fig. 1(c). The ground state can be completely characterized [22] by the probability density  $\langle \theta, \phi | \rho | \theta, \phi \rangle$ , where  $\rho = |\Psi\rangle\langle\Psi|$  is the density matrix. Results are shown in Fig. 1(b) and Figs. 2(a) and 2(b).

Numerical results for the gap are plotted in Fig. 2(c). The gap arises from tunneling between degenerate mean-field ground states. They can be approximated by taking Eq. (6) as a variational ground state of  $H_J$  with  $(\theta, \phi)$  as parameters. The value of  $\langle \theta, \phi | H_J | \theta, \phi \rangle$  is

$$E(\theta, \phi) \equiv -AJ^2 \left( \cos^2 \theta + 2 \frac{B}{B_c} \sin \theta \cos \phi \right), \quad (7)$$

neglecting smaller terms of order  $J$ . Degenerate minima of Eq. (7) occur at  $(\theta, \phi) = (\theta_0, 0)$  and  $(\theta, \phi) = (\pi - \theta_0, 0)$ , where  $\sin \theta_0 = B/B_c$ . The minima are separated by a tunnel barrier in the  $\theta$  direction with height  $V_0 = E(\pi/2, 0) - E(\theta_0, 0)$ . The transition amplitude  $\langle \theta | J_X | \pi - \theta \rangle$  causes tunneling between the degenerate minima, leading to a ground state that is a symmetric superposition separated in energy from the anti-symmetric superposition by a tunneling splitting. The value of the tunneling splitting can be computed using instanton methods [23] based on the path-integral representation of the propagator in the spin coherent state basis Eq. (6),

$$\begin{aligned} & \langle \theta_f, \phi_f | e^{-iH_J t} | \theta_i, \phi_i \rangle \\ &= \int_{(\theta_i, \phi_i)}^{(\theta_f, \phi_f)} \mathcal{D}\theta \mathcal{D}\phi \exp \left[ i \int_0^t dt' [J\dot{\phi}(1 - \cos \theta) - E(\theta, \phi)] \right]. \end{aligned} \quad (8)$$

<sup>3</sup>The terms  $J_X^2, J_Y^2$  are absent since they are prohibited here by momentum conservation.

<sup>4</sup>This transition bears similarity to the QPT between the normal and superradiant phase in the Dicke model.

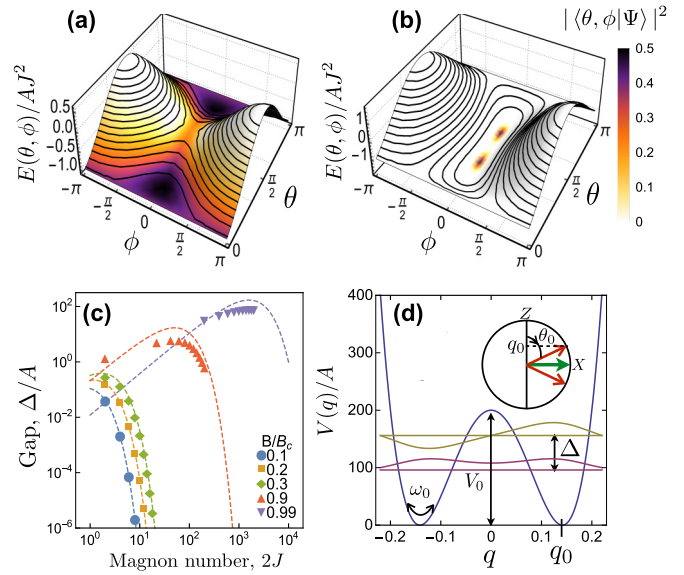


FIG. 2. Top panel: (surface plot) mean-field ground-state energy  $E(\theta, \phi)$  given in Eq. (7); (color density plot) ground-state probability density expressed in the pseudospin coherent-state basis given in Eq. (6). In (a)  $(B/B_c, J) = (0.3, 3)$  and (b)  $(B/B_c, J) = (0.9, 10^2)$ . Bottom panel: (c) Tunnel splitting in units of the interaction strength,  $\Delta/A$ , as a function of magnon number  $2J$ . Solid markers are computed by numerical diagonalization of Eq. (5) and dashed lines are computed from instanton formulas. (d) Effective quartic double-well potential,  $V(q)/A$ , in the polar pseudospin angle  $q = \cos \theta$  in the regime  $\epsilon \ll 1$  with  $(\epsilon, J) = (10^{-2}, 10^3)$ . Ground- and excited-state wave function computed from numerical diagonalization are also plotted.

To elucidate the results, we set  $\epsilon = 1 - B/B_c$  and separately consider  $\epsilon \approx 1$  and  $\epsilon \ll 1$ .

Far below the QPT, when  $B \ll B_c$  and  $\epsilon \approx 1$ , one finds that  $\sin \theta_0 \ll 1$ , so that  $V_0$  presents a high tunnel barrier in  $\theta$ . This leads to N00N-like ground states, well-localized near the poles as shown in Fig. 2(a), but with a very small tunnel splitting [5,24,25],

$$\Delta = A \frac{4J^{3/2}}{\sqrt{\pi}} \left( \frac{e}{2} \right)^{2J} \left( \frac{B}{B_c} \right)^{2J}. \quad (9)$$

The  $2J$  power-law dependence on  $B/B_c$  can be understood from perturbation theory, since the degeneracy of the  $J_Z^2$  eigenstates is lifted by the perturbation  $B J_X$  in the  $2J$ th order. As shown in Fig. 2(c), the tunnel splitting  $\Delta/A < 1$  is exponentially suppressed with magnon number. While this N00N-like state exhibits the entanglement that we seek, it will be difficult to prepare and observe since the tunnel splitting is too small.

To attain a larger tunnel splitting, we take  $B$  close to  $B_c$ , so that  $\epsilon \ll 1$ . We find that  $\theta_0 \approx \pi/2 - \sqrt{2\epsilon}$ . The classical minima at  $(\theta, \phi) = (\theta_0, 0)$  and  $(\theta, \phi) = (\pi - \theta_0, 0)$ , therefore, approach one another and the tunneling barrier height  $V_0 = A(J\epsilon)^2$  decreases. Quantum fluctuations in  $\phi$  are strongly suppressed, as shown in Fig. 2(b), and one can integrate out  $\phi$ . The result is an effective Lagrangian

$$L = \frac{mq^2}{2} - V(q),$$

where  $q \equiv \cos \theta$ ,  $m = 1/2A$  is an effective mass, and  $V(q) = V_0(q_0^2 - q^2)^2/q_0^4$  is a quartic double-well potential with minima at  $\pm q_0 = \pm\sqrt{2\epsilon}$  [5,23]. This potential together with its ground- and excited-state wave functions is plotted in Fig. 2(d). The tunnel splitting is

$$\Delta = 4\sqrt{3}\omega_0\sqrt{\frac{S_0}{2\pi}}e^{-S_0},$$

where  $S_0 = (2J/3)(2\epsilon)^{3/2}$  is the instanton action and  $\omega_0 = 2JA\sqrt{2\epsilon}$  is the attempt frequency [5]. This tunnel splitting is compared to the numerical diagonalization in Fig. 2(c). For fixed  $\epsilon$ , we can maximize the gap by the scaling

$$J = J_{\max}(\epsilon) = 0.8\epsilon^{-3/2}, \quad (10)$$

which yields

$$\Delta_{\max} = 12\frac{J_0}{N}(1-\eta)J_{\max}^{2/3}. \quad (11)$$

Choosing  $\epsilon = 10^{-2}$ ,  $N = 10^4$  lattice sites, and  $2J = 10^3$  magnons, and noting typical values  $\eta = 0.8$  and  $J_0 = 5$  K [11], we find a splitting of  $\Delta = 120$  mK. This should be sufficiently large to permit initialization of the ground state in dilution refrigerator temperatures of 15 mK. For these parameters, the applied field requires tuning to precision of order  $\epsilon B_c = 0.1$  GHz, corresponding to a magnetic field of order mT, which should be experimentally feasible.

#### IV. MOMENTUM-SPACE ENTANGLEMENT

There are many ways to quantify the size or the number of particles involved in a superposition. One measure is the difference in the expectation value of an observable between the two superposed states [6]. Here,  $J_Z$  is a natural choice, since the ground state of our system is a superposition of states with large differences in  $\langle J_Z \rangle$ . The ground-state wave function plotted in Fig. 2(d) is a superposition of states localized at the minima  $\pm q_0$ . Although the distance between minima goes to zero as  $2q_0 = 2\sqrt{2\epsilon}$ , with the scaling Eq. (10), these states remain distinct as  $\langle J_Z \rangle \sim \pm Jq_0 = \pm J_{\max}(\epsilon)q_0 \sim \epsilon^{-1}$ . Thus, macroscopic entanglement seems plausible even as  $\epsilon$  shrinks. Below, we further quantify this entanglement with the entanglement entropy and a quantum metrological measure called quantum Fisher information.<sup>5</sup>

##### A. Entanglement entropy

In this section, we study the entanglement entropy as defined by the von Neumann entropy of the reduced density matrix (RDM) of  $2j$  magnons [26],

$$S_E(J, j) = -\text{tr}[\hat{\rho}_{2j} \log_2 \hat{\rho}_{2j}], \quad (12)$$

<sup>5</sup>We note that in this work we consider momentum-space entanglement, which is very different from real-space entanglement. For example, a product state in momentum space has entanglement in real space,  $|\mathbf{K}\rangle \otimes |-\mathbf{K}\rangle = \sum_{\mathbf{r}_1, \mathbf{r}_2} e^{i\mathbf{K}(\mathbf{r}_1 - \mathbf{r}_2)} |\mathbf{r}_1\rangle \otimes |\mathbf{r}_2\rangle$ , and a magnon condensate in single momentum mode can be considered macroscopically entangled in real space [30].

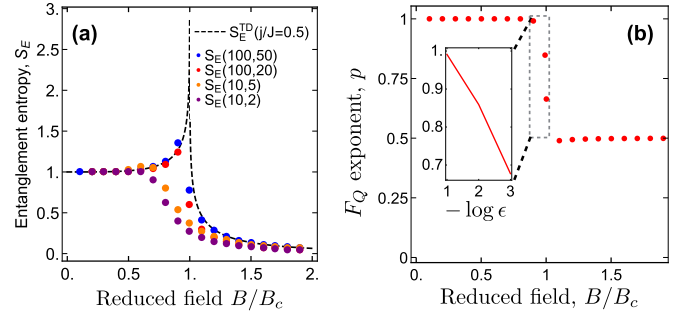


FIG. 3. (a) Momentum-space entanglement entropy  $S_E$  as a function of the reduced field  $B/B_c$ . Dots show numerically computed values. The dashed line shows a theoretical curve in the thermodynamic limit. (b) The scaling exponent  $p$  of the quantum Fisher information  $F_Q$ , Eq. (16), as a function of  $B/B_c$ . The inset shows a logarithmic plot in the crossover region,  $\epsilon = 1 - B/B_c \leq 0.1$ .

where  $\hat{\rho}_{2j}$  is formed by tracing out  $2J - 2j$  magnons. Generally, the RDM matrix elements in any basis are given by [6]

$$(\rho_{2j})_{l_1 \dots l_{2j}}^{k_1 \dots k_{2j}} \equiv \frac{2(J-j)!}{2J!} \langle b_{k_1}^\dagger \dots b_{k_{2j}}^\dagger b_{l_1} \dots b_{l_{2j}} \rangle, \quad (13)$$

where  $k_i, l_i$  are the state labels for the  $i$ th particle, and the expectation value is taken in the ground state. Here,  $S_E$  can be more efficiently evaluated with the RDM in the occupation number representation in the momentum-space basis,<sup>6</sup> which is given by

$$\begin{aligned} (\tilde{\rho}_{2j})_n^m &\equiv \langle j, m | \hat{\rho}_{2j} | j, n \rangle \\ &= \sqrt{\binom{2j}{m} \binom{2j}{n}} \frac{\langle (b_{-\mathbf{K}}^\dagger)^m (b_{\mathbf{K}}^\dagger)^{j-m} b_{-\mathbf{K}}^n b_{\mathbf{K}}^{j-n} \rangle}{2J! / 2(J-j)!}. \end{aligned} \quad (14)$$

The entanglement entropy for several values of  $J$  and  $j$  for finite  $J$  is plotted in Fig. 3(a). At  $\epsilon \simeq 1$  ( $B \ll B_c$ ),  $S_E = 1$  as expected for a N00N state, where mainly two states are occupied, while at  $\epsilon \ll 0$  ( $B \gg B_c$ ),  $S_E \rightarrow 0$ , where the ground state approaches an eigenstate of  $J_X$ . Near the quantum critical point  $B \rightarrow B_c$ , where we propose working,  $S_E$  is enhanced. In fact, a cusplike peak is apparent [18,19]. In the thermodynamic limit, the peak becomes a logarithmic divergence, as shown by computing  $S_E$  in a  $1/J$  expansion [20]. The leading term is given by

$$S_E^{(\text{TD})} = \frac{x+1}{2} \log_2 \left( \frac{x+1}{2} \right) - \frac{x-1}{2} \log_2 \left( \frac{x-1}{2} \right) + c, \quad (15)$$

where  $x = \alpha^{-1/2} \sqrt{[\alpha r + (1-r)][\alpha(1-r) + r]}$ ,  $r = j/J$ ; for  $\epsilon < 0$ ,  $\alpha = \sqrt{\epsilon/(\epsilon-1)}$ , and  $c = 1$ , while for  $\epsilon > 0$ ,  $\alpha = \sqrt{(\epsilon-2)\epsilon}$ , and  $c = 0$ . In the limit  $\epsilon \rightarrow 0$ ,  $S_E^{(\text{TD})} \sim -(1/4) \ln |\epsilon|$ , so the QCP is signaled by a logarithmic

<sup>6</sup>Since the nonzero eigenvalues of Eqs. (13) and (14) are the same, either can be used to calculate the entanglement entropy.

divergence. This analytical result in the thermodynamic limit is also plotted in Fig. 3(a).

The behavior of  $S_E$  confirms the presence of entanglement in our ground state, but it is an imprecise measure, as its value is affected by entanglement due to symmetrization of the wave function, which is nonzero even for a single Fock state  $|J, m\rangle$ . The correct interpretation of this type of entanglement and its potential for use in quantum information is still a subject of debate [27,28].

### B. Quantum Fisher information

In this section, we study an entanglement measure called quantum Fisher information that determines the ability of the system to find use in precision quantum metrology and show that it can be measured experimentally. If a relative phase  $\phi$  is accumulated between the condensate states  $|\pm\mathbf{K}\rangle$ , leading to the state  $|\Psi(\phi)\rangle = e^{i\phi J_Z}|\Psi\rangle$ , a measurement of  $\phi$  will have a minimum phase estimation error  $\delta\phi$  bounded by the quantum Cramer-Rao bound  $\delta\phi_{\min} = 1/\sqrt{F_Q}$ , where  $F_Q$  is the quantum Fisher information [29], which is given by

$$F_Q = 4[\langle\Psi'(\phi)|\Psi'(\phi)\rangle - |\langle\Psi'(\phi)|\Psi(\phi)\rangle|^2] = \langle\Delta J_Z^2\rangle,$$

where  $\Delta J_Z \equiv J_Z - \langle J_Z\rangle$ , and this result holds for pure states. For example, a NOON state would yield  $\langle\Delta J_Z^2\rangle = J^2$ , while the cat state we propose with the parameter values  $\epsilon = 10^{-2}$  and  $2J = 10^3$  has  $\langle\Delta J_Z^2\rangle = 58.9$ .

In quantum metrology, one is interested in how precision scales with the number particles used for the measurement. Defining the scaling exponent  $p$  by [30]

$$\sqrt{\langle\Delta J_Z^2\rangle} = O(J^p), \quad (16)$$

we have  $\delta\phi_{\min} \propto J^{-p}$ . Therefore,  $p$  measures the scaling of precision with magnon number;  $p = 0.5$  is the so-called standard quantum limit, while  $p = 1$  is the Heisenberg limit, showing quantum enhanced precision. Figure 3(a) plots a numerical fit to  $p$  as a function of  $B/B_c$ . We find that  $p = 1$  in the range  $0 < B/B_c \lesssim 0.9$ , and  $p = 0.5$  at  $B/B_c \gg 1$ , where the ground state  $|\theta = \pi/2, \phi = 0\rangle$  is separable when written in terms of  $b_{\mathbf{K}}^\dagger$  and  $b_{-\mathbf{K}}^\dagger$ . For  $0.9 \lesssim B/B_c < 1$  ( $\epsilon < 0.1$ ), we find  $p$  goes as  $1.15 + 0.16 \log \epsilon$  as shown in the inset of Fig. 3(b). For the cat state we propose,  $B/B_c = 0.99$  and  $p \simeq 0.85$ , which is a significant amount of entanglement.

For experimental measurement, the  $J_Z$  variance can be related to a spin correlation function that can be probed with neutron scattering [15],

$$\begin{aligned} \langle\Delta J_Z^2\rangle &= J(J+1) - \langle J_X^2\rangle - \langle J_Y^2\rangle \\ &= J^2 - N\langle S_{\mathbf{Q}}^z S_{-\mathbf{Q}}^z\rangle_c, \end{aligned} \quad (17)$$

where we used  $\langle J_Z\rangle = 0$ , and  $\langle \dots \rangle_c$  denotes the condensate contribution to the expectation value. The order parameter  $\langle J_X\rangle$  of the QPT sets the amplitude of modulation of a spin-density wave in  $S_{\mathbf{r}}^z$ ,

$$\langle \hat{n}_{\mathbf{r}} \rangle = \langle S_{\mathbf{r}}^z \rangle + S = 2J + 2\langle J_X \rangle \cos \mathbf{Q} \cdot \mathbf{r},$$

which can be measured by Brillouin light scattering [7,31].

### V. DECOHERENCE

The Hamiltonian Eq. (5) is formally identical to a model for a uniaxial ferromagnet in a transverse field [5,24,25]. However, in that case, coherence is highly vulnerable to dephasing from Zeeman coupling to low-frequency magnetic field noise [5]. For a system starting in the ground state, such noise will lead to excitations via a large  $J_Z$  matrix element to the first excited state. In contrast, one of the remarkable aspects of this magnon system is its robust coherence. Ambient magnetic field noise perturbs the pseudospin  $J_X$  term in the magnon Hamiltonian, which should have a negligible effect on the ground state because its  $J_X$  matrix element to the first excited state is very small. A  $J_Z$  dephasing term would require a highly nontrivial interaction capable of differentiating between spin textures of opposite chirality.

The ground state of our system should be much more robust against particle loss than, say, a NOON state [32]. Still, we expect the lifetime of the quantum state to be determined by magnon loss due to uniaxial U(1) symmetry-breaking terms that arise generically from Dzyaloshinsky-Moriya interactions, magnetic crystalline anisotropy, and dipolar interactions. Only an in-plane Dzyaloshinsky-Moriya vector would break uniaxial symmetry, but such a vector is forbidden here by inversion symmetry in the plane. The crystalline anisotropy Hamiltonian is also severely restricted by inversion symmetry; uniaxial symmetry-breaking terms only arise at fourth order in the spin operators. Thus the dominant term is the dipolar interaction, scaling as  $V_d = g^2 \mu_B^2 / a_0^3$  [7], that leads to many-body scattering and magnon decay [33]. For an estimate of the decay rate, we consider three-magnon scattering. Energy conservation forbids spontaneous emission out of the zero-energy condensate manifold,<sup>7</sup> but transfer of magnons between  $\{\pm\mathbf{K}\}$  is allowed by the umklapp process  $|\mathbf{K}\rangle \rightarrow |-\mathbf{K}\rangle + |-\mathbf{K}\rangle$  because  $\mathbf{G} = 3\mathbf{K}$  is a reciprocal-lattice vector. The rate of this process goes like  $\gamma_{\mathbf{K}}^{(3)} \sim 2\pi |v^{(3)}|^2 D_{\mathbf{K}}(0)$ , where  $v^{(3)} \sim V_d / \sqrt{N}$ , and  $D_{\mathbf{K}}(\omega) = \sum_{\mathbf{q}} \delta(\omega - \omega_{\mathbf{q}} - \omega_{\mathbf{K}-\mathbf{q}})$  is the density of states of the two-magnon continuum. In two dimensions,  $D_{\mathbf{K}}(\omega)$  scales as  $\mathcal{A}m/\pi$ , where  $\mathcal{A} \sim Na_0^2$  is the area and  $m \sim 1/J_0 a_0^2$  is the magnon effective mass. For a typical lattice constant  $a_0 = 0.7$  nm [34],  $V_d \sim 10$  mK, so the rate scales as  $\gamma_{\mathbf{K}}^{(3)} \sim V_d^2 / J_0 \sim 10^{-3}$  mK. This is much smaller than the energy scale set by the gap  $\Delta$ .

### VI. CONCLUSION AND OUTLOOK

This work presents a proposal for establishing robust momentum-space entanglement in the ground state of condensed magnons in a quasi-two-dimensional canted  $XY$  antiferromagnet on a triangular lattice. The proposed magnon Schrödinger-cat state is established by tuning parameters near a quantum phase transition, where the entanglement entropy is strongly enhanced. It was shown that the degree of entanglement as defined by the quantum Fisher information can be measured experimentally with neutron scattering.

<sup>7</sup>We assume that phonons, which could provide another decay channel, are frozen out at the low temperatures considered here.

In light of recent experiments in incorporating magnons in yttrium-iron garnet (YIG) in circuit quantum electrodynamics [35], it would be interesting to consider whether the entanglement explored here may also be engineered

in a quasiequilibrium magnon condensate in YIG. The potential for such a driven dissipative quantum phase that supports many-body entanglement warrants further study.

- 
- [1] E. Schrödinger, *Naturwissenschaften* **23**, 807 (1935).
- [2] Y.-A. Chen, X.-H. Bao, Z.-S. Yuan, S. Chen, B. Zhao, and J.-W. Pan, *Phys. Rev. Lett.* **104**, 043601 (2010); J. A. Jones, S. D. Karlen, J. Fitzsimons, A. Ardavan, S. C. Benjamin, G. A. D. Briggs, and J. J. L. Morton, *Science* **324**, 1166 (2009).
- [3] M. Bergmann and P. van Loock, *Phys. Rev. A* **94**, 012311 (2016).
- [4] J. Esteve, C. Gross, A. Weller, S. Giovanazzi, and M. K. Oberthaler, *Nature (London)* **455**, 1216 (2008); M. A. Leung, K. W. Mahmud, and W. P. Reinhardt, *Mol. Phys.* **110**, 801 (2012); H. W. Lau, Z. Dutton, T. Wang, and C. Simon, *Phys. Rev. Lett.* **113**, 090401 (2014); J. I. Cirac, M. Lewenstein, K. Mølmer, and P. Zoller, *Phys. Rev. A* **57**, 1208 (1998); T. D. Stanescu, B. Anderson, and V. Galitski, *ibid.* **78**, 023616 (2008); A. Nunnenkamp, A. M. Rey, and K. Burnett, *ibid.* **77**, 023622 (2008); D. W. Hallwood, T. Ernst, and J. Brand, *ibid.* **82**, 063623 (2010); D. W. Hallwood and J. Brand, *ibid.* **84**, 043620 (2011).
- [5] E. M. Chudnovsky and J. Tejada, *Macroscopic Quantum Tunneling of the Magnetic Moment (Cambridge Studies in Magnetism)* (Cambridge University Press, Cambridge, 2005); W. Wernsdorfer, E. Bonet Orozco, K. Hasselbach, A. Benoit, D. Mailly, O. Kubo, H. Nakano, and B. Barbara, *Phys. Rev. Lett.* **79**, 4014 (1997); H.-B. Braun, J. Kyriakidis, and D. Loss, *Phys. Rev. B* **56**, 8129 (1997); A. Garg and G.-H. Kim, *Phys. Rev. Lett.* **63**, 2512 (1989).
- [6] J. R. Friedman, V. Patel, W. Chen, S. K. Tolpygo, and J. E. Lukens, *Nature (London)* **406**, 43 (2000); J. I. Korsbakken, F. K. Wilhelm, and K. B. Whaley, *Phys. Scr.* **2009**, 014022 (2009); J. I. Korsbakken, K. B. Whaley, J. Dubois, and J. I. Cirac, *Phys. Rev. A* **75**, 042106 (2007); F. Marquardt, B. Abel, and J. von Delft, *ibid.* **78**, 012109 (2008).
- [7] P. Nowik-Boltyk, O. Dzyapko, V. E. Demidov, N. G. Berloff, and S. O. Demokritov, *Sci. Rep.* **2**, 482 EP (2012); S. O. Demokritov, V. E. Demidov, O. Dzyapko, G. A. Melkov, A. A. Serga, B. Hillebrands, and A. N. Slavin, *Nature (London)* **443**, 430 (2006); I. S. Tupitsyn, P. C. E. Stamp, and A. L. Burin, *Phys. Rev. Lett.* **100**, 257202 (2008).
- [8] V. Zapf, M. Jaime, and D. Batista, *Rev. Mod. Phys.* **86**, 563 (2014).
- [9] F. Li, W. M. Saslow, and V. L. Pokrovsky, *Sci. Rep.* **3**, 1372 (2013).
- [10] A. J. Leggett, *Rev. Mod. Phys.* **73**, 307 (2001).
- [11] T. Nikuni and H. Shiba, *J. Phys. Soc. Jpn.* **64**, 3471 (1995); **62**, 3268 (1993).
- [12] T. Radu, H. Wilhelm, V. Yushankhai, D. Kovrizhin, R. Coldea, Z. Tylczynski, T. Lühmann, and F. Steglich, *Phys. Rev. Lett.* **95**, 127202 (2005); D. Yamamoto, G. Marmorini, and I. Danshita, *ibid.* **112**, 127203 (2014); R. Coldea, D. A. Tennant, K. Habicht, P. Smeibidl, C. Wolters, and Z. Tylczynski, *ibid.* **88**, 137203 (2002).
- [13] E. Altman, W. Hofstetter, E. Demler, and M. D. Lukin, *New J. Phys.* **5**, 113 (2003); L. He, Y. Li, E. Altman, and W. Hofstetter, *Phys. Rev. A* **86**, 043620 (2012); J. Simon, W. S. Bakr, R. Ma, M. E. Tai, P. M. Preiss, and M. Greiner, *Nature (London)* **472**, 307 (2011); C. H. Wong and R. A. Duine, *Phys. Rev. A* **88**, 053631 (2013); *Phys. Rev. Lett.* **110**, 115301 (2013).
- [14] A. A. Houck, D. I. Schuster, J. M. Gambetta, J. A. Schreier, B. R. Johnson, J. M. Chow, L. Frunzio, J. Majer, M. H. Devoret, S. M. Girvin, and R. J. Schoelkopf, *Nature (London)* **449**, 328 (2007); K. L. Hur, L. Henriët, A. Petrescu, K. Plekhanov, G. Roux, and M. Schiró, *C. R. Phys.* **17**, 808 (2016); M. Schiró, M. Bordyuh, B. Öztop, and H. E. Türeci, *Phys. Rev. Lett.* **109**, 053601 (2012); M. Dalmonte, S. I. Mirzaei, P. R. Muppalla, D. Marcos, P. Zoller, and G. Kirchmair, *Phys. Rev. B* **92**, 174507 (2015).
- [15] C. Kittel, *Quantum Theory of Solids* (Wiley, New York, 1987).
- [16] T. Giamarchi, C. Rugg, and O. Tchernyshyov, *Nat. Phys.* **4**, 198 (2008); Y. Kamiya and C. D. Batista, *Phys. Rev. X* **4**, 011023 (2014); A. A. Aczel, Y. Kohama, M. Jaime, K. Ninios, H. B. Chan, L. Balicas, H. A. Dabkowska, and G. M. Luke, *Phys. Rev. B* **79**, 100409 (2009); T. Nikuni, M. Oshikawa, A. Oosawa, and H. Tanaka, *Phys. Rev. Lett.* **84**, 5868 (2000).
- [17] J. Sakurai, *Modern Quantum Mechanics* (Addison-Wesley, Reading, MA, 1994).
- [18] S. Dusuel and J. Vidal, *Phys. Rev. B* **71**, 224420 (2005).
- [19] J. I. Latorre, R. Orús, E. Rico, and J. Vidal, *Phys. Rev. A* **71**, 064101 (2005).
- [20] T. Barthel, S. Dusuel, and J. Vidal, *Phys. Rev. Lett.* **97**, 220402 (2006).
- [21] R. Botet and R. Jullien, *Phys. Rev. B* **28**, 3955 (1983).
- [22] B. C. Sanders, *Phys. Rev. A* **40**, 2417 (1989).
- [23] A. Garg and G.-H. Kim, *Phys. Rev. B* **45**, 12921 (1992).
- [24] E. M. Chudnovsky and L. Gunther, *Phys. Rev. Lett.* **60**, 661 (1988).
- [25] D. A. Garanin, *J. Phys. A* **24**, L61 (1991).
- [26] R. Paškauskas and L. You, *Phys. Rev. A* **64**, 042310 (2001).
- [27] H. M. Wiseman and J. A. Vaccaro, *Phys. Rev. Lett.* **91**, 097902 (2003).
- [28] S. Sciara, R. Lo Franco, and G. Compagno, *Sci. Rep.* **7**, 44675 (2017).
- [29] S. L. Braunstein and C. M. Caves, *Phys. Rev. Lett.* **72**, 3439 (1994).
- [30] T. Morimae, A. Sugita, and A. Shimizu, *Phys. Rev. A* **71**, 032317 (2005).
- [31] A. S. Borovik-Romanov and N. M. Kreines, *J. Appl. Phys.* **53**, 8157 (1982); F. Ganot, C. Dugautier, P. Moch, and J. Nouet, *J. Phys. C* **15**, 801 (1982); J. Milano and M. Grimsditch, *Phys. Rev. B* **81**, 094415 (2010).
- [32] U. Dorner, R. Demkowicz-Dobrzanski, B. J. Smith, J. S. Lundeen, W. Wasilewski, K. Banaszek, and I. A. Walmsley, *Phys. Rev. Lett.* **102**, 040403 (2009); J. Huang, X. Qin, H. Zhong, Y. Ke, and C. Lee, *Sci. Rep.* **5**, 17894 (2015).

- [33] M. E. Zhitomirsky and A. L. Chernyshev, *Rev. Mod. Phys.* **85**, 219 (2013).
- [34] K. Adachi, N. Achiwa, and M. Mekata, *J. Phys. Soc. Jpn.* **49**, 545 (1980).
- [35] X. Zhang, C.-L. Zou, N. Zhu, F. Marquardt, L. Jiang, and H. X. Tang, *Nat. Commun.* **6**, 8914 (2015); K. Nakata, K. A. van Hoogdalem, P. Simon, and D. Loss, *Phys. Rev. B* **90**, 144419 (2014); Y. Tabuchi, S. Ishino, A. Noguchi, T. Ishikawa, R. Yamazaki, K. Usami, and Y. Nakamura, *Science* **349**, 405 (2015); Y. Tabuchi, S. Ishino, T. Ishikawa, R. Yamazaki, K. Usami, and Y. Nakamura, *Phys. Rev. Lett.* **113**, 083603 (2014).